

## H<sub>2</sub>/CO<sub>2</sub> Separation Characteristics of $\gamma$ -Al<sub>2</sub>O<sub>3</sub> Membrane by Aging Stage in Sol-Gel Process

Seung-Joon Yoo<sup>†</sup>, Jung-Woon Lee\*, Un-Yeon Hwang\*, Hyung-Sang Park\*, Dal-Ryung Park\*\*, Hee-Dong Jang\*\*\* and Ho-Sung Yoon\*\*\*

Faculty of Environmental and Chemical Engineering, Seonam University

\*Department of Chemical Engineering, Sogang University

\*\*Gas R&D Center, Division of Gas Utilization, Korea Gas Corporation

\*\*\*Division of Minerals Utilization and Materials,

Korea Institute of Geology, Mining & Materials

(Received 10 December 1999 • accepted 7 April 2000)

**Abstract**— $\gamma$ -AlO(OH) sol solution was prepared by aluminum isopropoxide as an initial material.  $\gamma$ -Al<sub>2</sub>O<sub>3</sub> membrane on the  $\alpha$ -Al<sub>2</sub>O<sub>3</sub> support was continuously made through coating and thermal treatment from the  $\gamma$ -AlO(OH) sol. Previous work [Yoo et al., 1997] has shown that the aging stage in the sol preparation process mainly affects the characterization of  $\gamma$ -Al<sub>2</sub>O<sub>3</sub> particles as well as  $\gamma$ -AlO(OH) sol. Based on this fact, the  $\gamma$ -Al<sub>2</sub>O<sub>3</sub> membrane was prepared with two aging conditions in the present study. The separation characteristics experiment of the H<sub>2</sub>/CO<sub>2</sub> mixture was performed on these membranes. As a result of the study, the mechanism of gas transport on the two membranes was proved as Knudsen diffusion. The ideal separation factor was reached at the value of the calculated Knudsen separation factor; however, permeability increased and selectivity decreased according to the aging.

Key words: Aging, Microstructure,  $\gamma$ -AlO(OH) Sol,  $\gamma$ -Al<sub>2</sub>O<sub>3</sub> Membrane, Permeability, Selectivity

### INTRODUCTION

Along with the development of industries such as chemical, advanced materials, energy and electronics, the emission of environmental pollution gases such as NO<sub>x</sub>, SO<sub>x</sub> and CO<sub>x</sub> into the atmosphere tends to increase year by year [Paul et al., 1994], leading to climate changes all over the world. The damage caused by such climate change is not just limited to a certain country, but has become a serious global problem. Accordingly, international societies have set many emission limits for these pollution gases. The limits of concentration regulation have also been tightened strictly. Yet even with such possible damage, all possible technologies must be developed because countries cannot stop industrial activities. Technological development of separation purification and new clean energy are included in these technologies.

Membrane technology is very simple and economical in contrast to other technologies such as adsorption/desorption and solvent extraction among the available separation purification technologies. The membranes are classified into organic, inorganic, and composite membranes according to the type of material. Ceramic membranes, which were selected as the inorganic material, have great potential for the separation of gases at high temperature and some advantages different from organic membranes. For example, they can diminish latent heat loss caused by the phase change in high-temperature gas separation, and can directly use permeated high-temperature gas to the next process without sensible heat loss. Ceramic membranes can withstand temperatures above 1,000 °C. Moreover, the resistance to chemicals makes them virtually im-

mune to various solvents such as acids, alkalies, and detergents. Their mechanical strength can also withstand pressures above 10 atm. For these reasons, the use of ceramic membranes has continuously increased by more than 10% annually. Although the performance characteristics are highly attractive to many processing industries, ceramic membranes have not been extensively used because of their high cost and questionable control in pore size distribution. Recent sol-gel technology, however, can be an alternative to solve these problems. The sol-gel technology permits mass production of the ceramic membrane which has a uniform pore size distribution and is economically viable [Chan and Brownstein, 1991].

In the present study, we selected the  $\gamma$ -Al<sub>2</sub>O<sub>3</sub> membrane among the ceramic membranes and prepared the  $\gamma$ -Al<sub>2</sub>O<sub>3</sub> membrane through the  $\gamma$ -AlO(OH) sol preparation stage using aluminum isopropoxide as the initial material. In general, the characterization of the  $\gamma$ -Al<sub>2</sub>O<sub>3</sub> membrane is sensitively affected by the transition stages from aluminum isopropoxide to  $\gamma$ -AlO(OH) sol,  $\gamma$ -AlO(OH) sol to gel and the gel to  $\gamma$ -Al<sub>2</sub>O<sub>3</sub> particles. The research to control  $\gamma$ -Al<sub>2</sub>O<sub>3</sub> particles characterization owing to the  $\gamma$ -AlO(OH) sol preparation stage, however, was very deficient than other transition stages until now. In these circumstance, previous works [Yoo et al., 1997, 1998] have shown that the microstructure characterization of the  $\gamma$ -Al<sub>2</sub>O<sub>3</sub> particle has been affected by the aging stage mainly among the various sol process stages such as hydrolysis, polymerization/condensation, aging, and peptization. At that time, the conditions of other stages such as drying and calcination were constantly maintained in order to investigate effects of the aging stage. In the previous works, the  $\gamma$ -Al<sub>2</sub>O<sub>3</sub> particles showed change of microstructure characterization of the  $\gamma$ -Al<sub>2</sub>O<sub>3</sub> particles owing to aging time such as 6.2 nm (average pore diameter) and 254 m<sup>2</sup>/g

<sup>†</sup>To whom correspondence should be addressed.

E-mail: sjyoo@tiger.seonam.ac.kr

(specific surface area) after being calcined at 600 °C in the case of 1 hr aging, and 18.0 nm (average pore diameter) and 186 m<sup>2</sup>/g specific surface area) in case of 72 hrs aging.

In the present study, we performed the separation characteristics experiments on hydrogen and carbon dioxide mixture in order to evaluate the performance of the  $\gamma$ -Al<sub>2</sub>O<sub>3</sub> membranes prepared by these two different aging conditions.

This research has focused on the optimum condition for the  $\gamma$ -Al<sub>2</sub>O<sub>3</sub> membrane by sol-gel method. Needless to say, noble metals such as palladium, platinum and rhodium must be impregnated on the sol in order to obtain selective membrane. And much effort has been made to improve the selectivity of porous inorganic membrane via surface diffusion generated by the pore modification [Chai et al., 1994; Lee et al., 1995; So et al., 1999].

## EXPERIMENTAL

Fig. 1 is a schematic flow diagram for the  $\gamma$ -Al<sub>2</sub>O<sub>3</sub> membrane preparation by the sol-gel method. Aluminum isopropoxide (Al(OC<sub>3</sub>H<sub>7</sub>)<sub>3</sub>, Fluka Chemie, AG) was used as an alkoxide precursor. The reactants ratio was kept at 100 mol water per 1 mol aluminum isopropoxide as proposed by Yoldas [Yoldas, 1973, 1975a, b, c]. The chemical reaction time proceeded for 30 mins at 90 °C under open condition of reactor. The  $\gamma$ -AlO(OH) precipitated solution was prepared according to the change of aging times at 96 °C in succession after the chemical reaction. To obtain a stabilized  $\gamma$ -AlO(OH) sol, HCl (Merck, 32%) was added 0.07 mole ratio HCl/Al as an acidic electrolyte in  $\gamma$ -AlO(OH) precipitated solution and peptization was performed under vigorous stirring for 24 hrs at 96 °C.

Fig. 2 is a photograph of the tubular porous  $\alpha$ -Al<sub>2</sub>O<sub>3</sub> support used in this experiment. The support is a commercial product man-

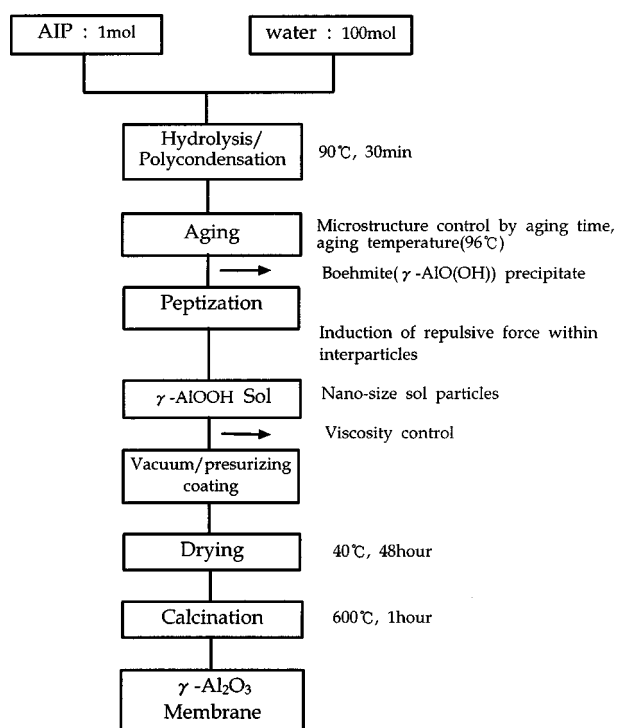


Fig. 1. Flow diagram of experimental procedure.

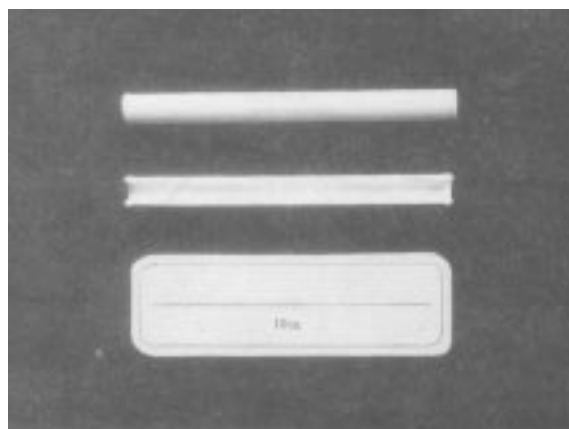


Fig. 2. Photograph of porous  $\alpha$ -Al<sub>2</sub>O<sub>3</sub> support.

Table 1. Specification of  $\alpha$ -Al<sub>2</sub>O<sub>3</sub> support

Type	Content
Manufacturer	Dongsu Ind. Co.
Raw material	$\alpha$ -Al <sub>2</sub> O <sub>3</sub>
Average pore diameter (4V/A)	0.145 $\mu$ m
Total pore area	6.568 m <sup>2</sup> /g
Porosity	48.01%
Outside diameter	10.00 mm
Inside diameter	8.00 mm

ufactured by Dongsu Industrial Co. (Korea) which has an average pore diameter of 145 nm and porosity 48.01% as shown in Table 1. The support was sealed by glaze, except for the constant area, 3 cm<sup>2</sup> ( $D_o=10.65$  mm,  $D_i=7.3$  mm,  $l_o=10$  mm,  $l_i=12$  mm) of the middle part in order to measure permeability and selectivity on the constant permeation area and sintered during 1 hr at 1,200 °C. The glaze consists of silica and feldspar for the most part as a glaze of limestone extraction as shown in Table 2.

Using the stable  $\gamma$ -AlO(OH) sol obtained after peptization, we coated the sol on tubular  $\alpha$ -Al<sub>2</sub>O<sub>3</sub> support by a vacuum/pressurizing coating apparatus devised by our researchers. Fig. 3 shows a schematic diagram of the vacuum/pressurizing coating apparatus devised for sol coating. The  $\alpha$ -Al<sub>2</sub>O<sub>3</sub> support was inserted into the inside of cell. After the top port was sealed tightly, the cell maintained at 3 cmHg for 1 hr by vacuum pump.  $\gamma$ -AlO(OH) sol of proper amount was flowed through NV2, the cell was pressurized to 1.5 atm slowly from the air bomb in order for the  $\gamma$ -AlO(OH) sol to penetrate into the  $\alpha$ -Al<sub>2</sub>O<sub>3</sub> support. And the thickness of the

Table 2. Composition of glaze

Components	Content (wt%)
SiO <sub>2</sub>	25
Feldspar	31
Kaolin	8
Limestone	15
Dolomite	5
ZrO <sub>2</sub>	10
ZnO	3
Frit	3

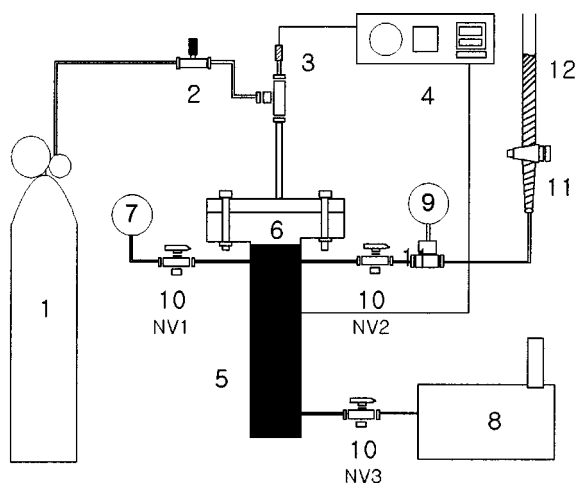


**Fig. 3. Schematic diagram for vacuum/pressurizing coating apparatus.**

- |                            |                              |
|----------------------------|------------------------------|
| 1. N <sub>2</sub> cylinder | 8. Vacuum pump               |
| 2. Metering valve          | 9. Pressure gauge            |
| 3. Thermocouple            | 10. Needle valves: NV1; NV2; |
| 4. Temperature controller  | NV3                          |
| 5. Heating coil            | 11. Burette                  |
| 6. Module                  | 12. Sol solution             |
| 7. Vacuum gauge            |                              |

coated layer was controlled by sedimentation rate caused by gravitational force like pulling rate in the dip coating. The thickness of the membranes was in the range of 2-5  $\mu\text{m}$  by one time coating in this experiment. The viscosity of sol was controlled to 1.5 cP by the control of the concentration of the sol.

The coated membrane layer was dried slowly over the 48 hrs

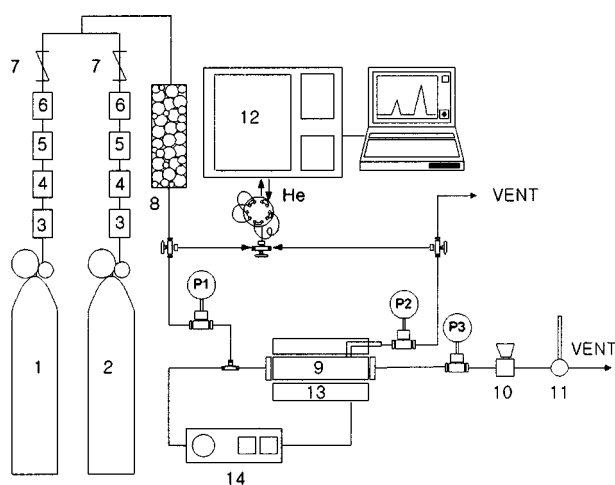


**Fig. 4. Schematic diagram for separation characteristics apparatus.**

- |                                    |                              |
|------------------------------------|------------------------------|
| 1. CO <sub>2</sub> cylinder        | 8. Mixer with glass beads    |
| 2. H <sub>2</sub> cylinder         | 9. Housing                   |
| 3. Filter                          | 10. Back-pressure regulator  |
| 4. H <sub>2</sub> O trap           | 11. Bubble flow meter        |
| 5. O <sub>2</sub> trap             | 12. Gas chromatograph        |
| 6. Mass flow meter with controller | 13. Electric tubular furnace |
| 7. Check valve                     | 14. Temperature controller   |

under the condition of 40 °C and 55% relative humidity in the desiccator; the membrane was thermal-treated calcined up to 600 °C by temperature program under the air condition in a tubular furnace. For the  $\gamma\text{-Al}_2\text{O}_3$  membranes prepared by these various process stages, separation experiments were carried out on hydrogen and carbon dioxide mixture in order to evaluate the performance of the membranes.

Fig. 4 is a schematic diagram of the separation characteristics apparatus. Gas flow rate was controlled by a mass flow controller (Brooks, Model 5850C) and the permeated gas concentration was analyzed by a gas chromatograph (Young-lin G.C. 600D, TCD Detector, column material: Porapak Q, Oven Temp.; 150 °C, Injection Temp.; 150 °C, Detector Temp.; 170 °C, He flow rate: 20 cc/min), and permeability of permeated gas measured by a bubble flow meter. In the experiment of separation characteristics, the temperature of housing with  $\gamma\text{-Al}_2\text{O}_3$  membrane was maintained accurately under 323, 373, 423, and 473 K temperatures by a programmable PID temperature controller.

## RESULTS AND DISCUSSION

The  $\gamma\text{-AlO(OH)}$  sol particle is transformed to  $\alpha\text{-Al}_2\text{O}_3$  particle by thermal treatment above 1,200 °C temperature, but forms thermally stable  $\gamma\text{-Al}_2\text{O}_3$  between 450 °C and 900 °C. This  $\gamma\text{-Al}_2\text{O}_3$  particle has many excellent characterizations such as fine pores, high porosity, large specific surface area, and a thermally stable property. In this study, microstructure characterization of  $\gamma\text{-Al}_2\text{O}_3$  membrane was controlled by the change of aging in sol-gel method. The separation experiment was performed on the hydrogen and carbon dioxide mixture in order to evaluate performance of the synthesized  $\gamma\text{-Al}_2\text{O}_3$  membranes.

Fig. 5 is a SEM photograph of a fractural surface sealed by glaze. It shows that the support was sealed pores by glaze.

The viscosity of sol, which is determined by sol concentration, is the most important factor in the coating. It is essential to control sol viscosity, since the membrane thickness is determined by sol viscosity. Fig. 6 shows variation of the  $\gamma\text{-AlO(OH)}$  sol viscosity according to aging time. The viscosity of sol was analyzed by a Cannon-Fenske viscometer (Kusano Scientific Instrument Co. Ltd.). As a result of the experiment to remove cracks during dry-

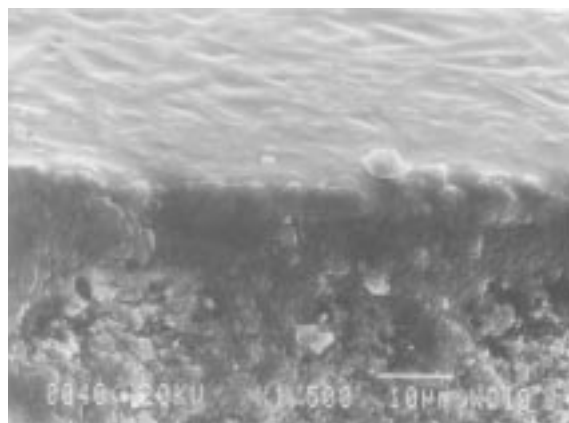


**Fig. 5. SEM photograph of fractural surface of  $\alpha\text{-Al}_2\text{O}_3$  support sealed by glaze.**

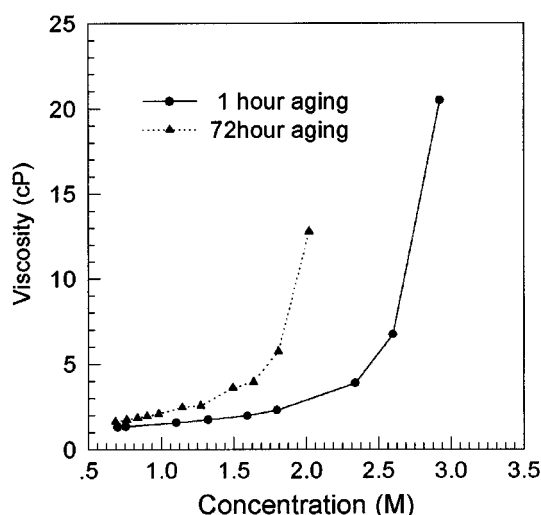


Fig. 6. Variation of viscosity on  $\gamma$ - $\text{AlO}(\text{OH})$  mole concentration.

ing, the range of appropriate sol viscosity was 1 to 1.5 cP. Accordingly, every sol viscosity was controlled to 1.5 cP and the coating was performed.

In spite of the one time vacuum/pressurizing coating, the pressure drop of the inside and outside of the membrane was maintained highly above 24 psi. This means that the affinity between the support and separation layer was increased, since the  $\gamma$ - $\text{AlO}(\text{OH})$  sol particles was penetrated into the pores of support surface.

The coated  $\gamma$ - $\text{AlO}(\text{OH})$  layer was transformed to high-temperature stable  $\gamma$ - $\text{Al}_2\text{O}_3$  membrane through the drying and calcination stages. These thermal treatment stages are of importance because cracks and warps occur under the stages.

In general, the cracks occur when the evaporation rate of the surface is faster than the subsurface during the drying. If the evaporation rate of the surface is faster than the subsurface, the sealed surface layer breaks when water in the subsurface evaporates outside. For this reason, the evaporation rate between surface and subsurface needs to be maintained constantly and slowly in order to remove occurrence of cracks. Accordingly, the drying proceeded slowly during 48 hrs at 40 °C and 55% relative humidity in this experiment.

After drying, the membrane was calcined during 1 hr at 600 °C under air condition using the tubular electric furnace. In this time, the air flow rate was 30 ml/min. Based on TGA analysis, the part of rapid weight loss (30-110 °C, 250-450 °C) increased slowly to 0.5 °C/min, and the other part increased to 2 °C/min. On the other hand, the rate of cooling also decreased to 1 °C/min like temperature increasing condition because the stage also accompanies cracks and warps.

Fig. 7(a) shows a photograph of  $\gamma$ - $\text{Al}_2\text{O}_3$  membrane calcined at 600 °C after coating using  $\gamma$ - $\text{AlO}(\text{OH})$  sol obtained by the constant aging condition (96 °C, 1 hr). We could show that the coated surface layer of separation membrane was uniformly formed. Fig. 7 (b) is a photograph of an enlarged fractural layer between support and coated  $\gamma$ - $\text{Al}_2\text{O}_3$  separation membrane showed in Fig. 7(a).

The  $\gamma$ - $\text{Al}_2\text{O}_3$  separation membrane prepared by the method stated above was used in order to measure permeation and selectivity of  $\gamma$ - $\text{Al}_2\text{O}_3$  membranes. The separation characteristics experiment

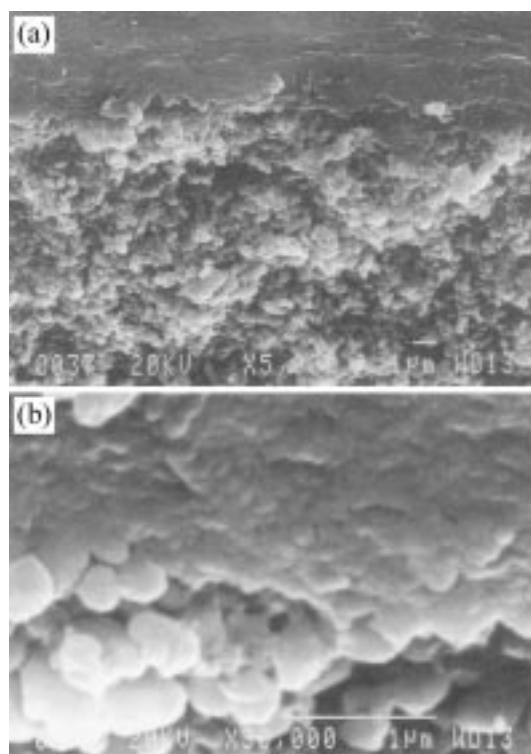


Fig. 7. SEM photographs of fractural surface of  $\gamma$ - $\text{Al}_2\text{O}_3$  membrane calcined at 600 °C: (a)  $\times 5,000$ ; (b)  $\times 30,000$ .

was performed on the  $\text{H}_2/\text{CO}_2$  mixture mixed by mole ratio of 10 to 1. Figs. 8 and 9 show the results of permeation measurement of pure hydrogen and carbon dioxide according to permeation temperature and pressure drop. As shown in Fig. 8, the permeability of all gases reached to a wide pressure drop range (3-24 psi) irrespective of the aging condition. This means that the vacuum/pressurizing coating method devised in this study is effective, and it shows that permeability is independent of pressure drop across the membrane. Fig. 9 shows that the relation between the permeability and square root of temperature is in inverse proportion according to

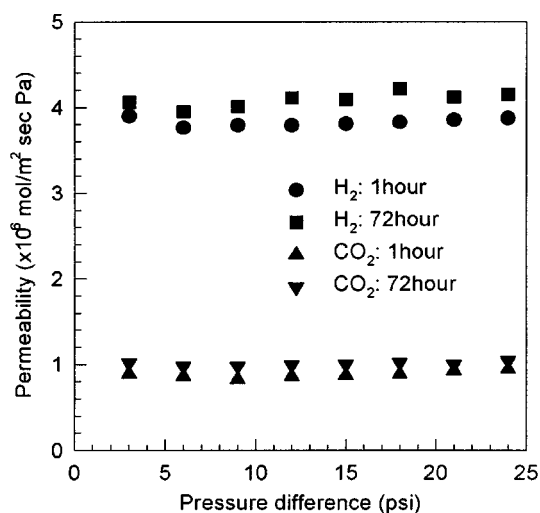


Fig. 8. Effect of pressure differences across the membrane on permeability of single gases for two different aging times at 473 K ( $\text{CO}_2$ : 50 ml/min,  $\text{H}_2$ : 100 ml/min).

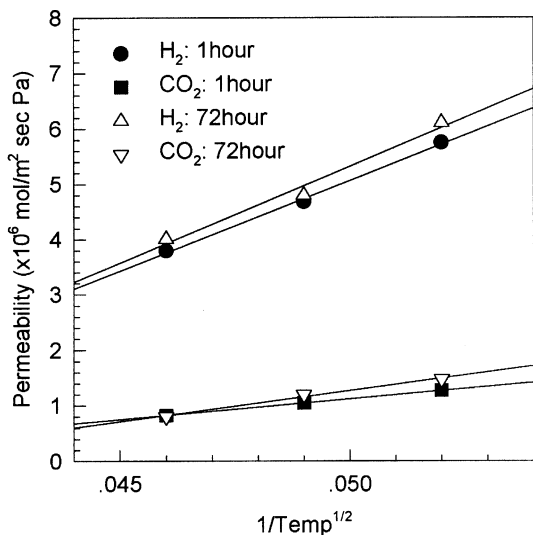


Fig. 9. Effect of the temperatures on permeability of single gases for two different aging times at 9 psi transpressure ( $\text{CO}_2$ : 50 ml/min,  $\text{H}_2$ : 100 ml/min).

increase of permeability temperature. The results indicate that gas separation through each prepared membrane was achieved mainly by Knudsen diffusion. And the permeability increased a little according to increase of aging time at 96 °C as shown in Fig. 8 and Fig. 9.

As gas transport is achieved by Knudsen diffusion, the ideal separation factor defines the permeability ratio of single gases ( $\text{H}_2/\text{CO}_2$ ). As shown in Fig. 10, the ideal separation factor almost reached the calculated Knudsen separation factor in this experiment. The ideal separation factor of  $\gamma\text{-Al}_2\text{O}_3$  membrane prepared by 1 hr aging, however, stands closer to the calculated separation factor than the  $\gamma\text{-Al}_2\text{O}_3$  membrane prepared by 72 hrs aging.

Fig. 11 presents selectivity analyzed by gas chromatography on the hydrogen and carbon dioxide mixture. It shows that the selectivity decreased according to the increase of aging time. And the selectivity increased according to increase of reaction temperature.

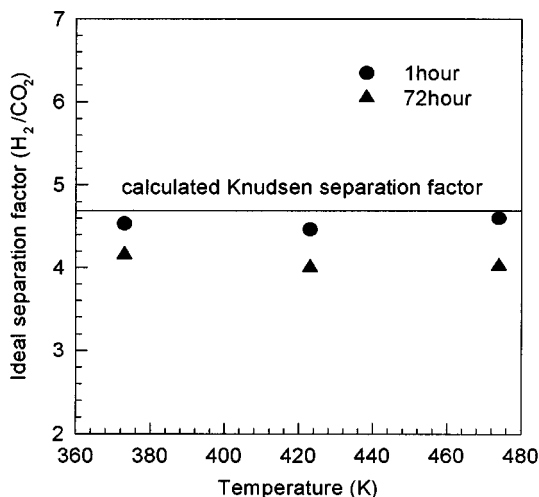


Fig. 10. The ideal separation factor of  $\text{CO}_2$  and  $\text{H}_2$  for two different aging times at 9 psi transpressure ( $\text{CO}_2$ : 10 ml/min,  $\text{H}_2$ : 100 ml/min).

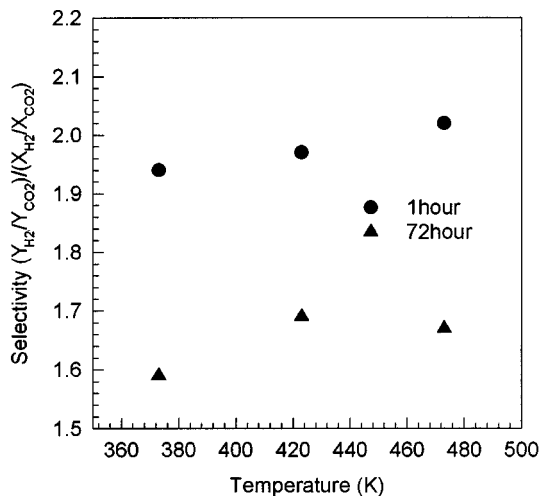


Fig. 11. The selectivity of  $\text{H}_2/\text{CO}_2$  mixture for two different aging times at 9 psi transpressure ( $\text{CO}_2$ : 10 ml/min,  $\text{H}_2$ : 100 ml/min).

This means that the molecular motion velocity of hydrogen was faster than carbon dioxide according to the increase of reaction temperature in the case of Knudsen diffusion. Therefore, selectivity of hydrogen on the carbon dioxide was improved according to the increase of reaction temperature.

And the selectivity of  $\gamma\text{-Al}_2\text{O}_3$  membrane prepared by 1 hr aging was improved compared to the  $\gamma\text{-Al}_2\text{O}_3$  membrane prepared by 72 hrs aging as shown in Fig. 11, because the aging changed the microstructure characterization of the membrane such as an increase of pore diameter and decrease of specific surface area.

## CONCLUSION

Separation characteristics of the  $\gamma\text{-Al}_2\text{O}_3$  membrane were studied on  $\text{H}_2/\text{CO}_2$  mixture according to the variation of aging condition in sol preparation. The permeability of the membranes was independent of pressure drop, and was in inverse proportion to the square root of reaction temperature. The ideal separation factor almost reached the calculated Knudsen separation factor. Accordingly, we could know that the gas transport mechanism of  $\gamma\text{-Al}_2\text{O}_3$  membranes prepared by the change of aging condition mainly followed Knudsen diffusion.

The selectivity decreased according to increase of aging time, and increased according to increase of reaction temperature. Therefore, we knew that the separation performance of  $\gamma\text{-Al}_2\text{O}_3$  membrane prepared by 1 hr aging time was better than the case of 72 hrs aging time for effective separation of gas mixture. In conclusion, the longer the aging time, the lower separation selectivity.

## NOMENCLATURE

- cP : centipoise [ $1.00 \times 10^{-3} \text{ kg/m} \cdot \text{s}$ ]
- M : mole concentration [mol/L]
- NV1, NV2, NV3 : first, second and third needle valves
- P1 : pressure at input side
- P2 : pressure at permeate side
- P3 : pressure at retentate side

TC : thermocouple

### Greek Letters

$\alpha$  : alpha-type

$\gamma$  : gamma-type

### REFERENCES

- Chai, M., Yamashita, Y., Machida, M., Eguchi, K. and Arai, H., "Preparation and Characterization of Metal-Dispersed Alumina Membranes for Selective Separation of Hydrogen," *J. Memb. Sci.*, **97**, 199 (1994).
- Chan, K. C. and Brownstein, A. K., "Ceramic Membranes-Growth Prospects and Opportunities," *Ceramic Bulletin*, **70**, 703 (1991).
- Lee, S.-J., Yang, S.-M. and Park, S. B., "Synthesis of Palladium Impregnated Alumina Membrane for Hydrogen Separation," *J. Memb. Sci.*, **96**, 223 (1994).
- Paul, J. and Pradier, C. M., "Carbon Dioxide Chemistry: Environmental Issue," THE ROYAL SOCIETY OF CHEMISTRY (1994).
- So, J.-H., Yoo, K.-Y., Yang, S.-M. and Park, S. B., "Preparations of Metal Impregnated Porous Inorganic Membranes for Hydrogen Separation by Multi-Step Pore Modification," *Korean J. Chem. Eng.*, **16**, 180 (1999).
- Yoldas, B. E., "Hydrolysis of Aluminum Alkoxides and Bayerite Conversion," *J. Appl. Chem. Biotechnol.*, **23**, 803 (1973).
- Yoldas, B. E., "A Transparent Porous Alumina," *Ceramic Bulletin*, **54**, 286 (1975a).
- Yoldas, B. E., "Alumina Gels that Form Porous Transparent Al<sub>2</sub>O<sub>3</sub>," *J. Mat. Sci.*, **10**, 1856 (1975b).
- Yoldas, B. E., "Alumina Sol Preparation from Alkoxides," *Amer. Ceram. Soc. Bull.*, **54**, 289 (1975c).
- Yoo, S.-J., Lee, J.-W., Hwang, U.-Y., Yoon, H.-S. and Park, H.-S., "Effect of Aging among  $\gamma$ -AlO(OH) Sol Preparation Steps Variables to Control Microstructure of  $\gamma$ -Al<sub>2</sub>O<sub>3</sub> Membrane," *HWAHAK KONGHAK*, **35**, 832 (1997).
- Yoo, S.-J., Lee, J.-W., Hwang, U.-Y., Yoon, H.-S. and Park, H.-S., "Effect of Peptization in  $\gamma$ -AlO(OH) Sol Preparation Process on Microstructure of  $\gamma$ -Al<sub>2</sub>O<sub>3</sub> Membrane," *HWAHAK KONGHAK*, **36**, 635 (1998).